

This paper by Professor Liviu Librescu was scheduled to be published in the December 2007 issue of the Journal of Ship Research. Professor Librescu was tragically killed in the shootings at Virginia Tech in April. He heroically blocked the door to his classroom while his students jumped out the window. His actions saved all but one.

Professor Librescu was a dedicated researcher and beloved teacher in the area of aeroelasticity, thermal stresses, and composites. This is the first paper Professor Librescu has published in the Journal of Ship Research. We are proud to have him as an author and extend our sympathies to his family, friends, and colleagues at Virginia Tech.

Implication of Nonclassical Effects on Dynamic Response of Sandwich Structures Exposed to Underwater and In-Air Explosions

Liviu Librescu,* Sang-Yong Oh,* and Jörg Hohe†

*Department of Engineering Science and Mechanics, Virginia Polytechnic Institute and State University, Blacksburg, Virginia, USA

†Fraunhofer Institut für Werkstoffmechanik, Freiburg, Germany

A study devoted to the dynamic response of sandwich panels to underwater and in-air explosions is presented. The study is carried out in the context of a geometrically nonlinear model of sandwich structures featuring anisotropic laminated face sheets and a transversely compressible orthotropic core. The unsteady pressure generated by the explosion and acting on the face of the sandwich panel includes the effect of the pressure wave transmission through the core. Its implications on the structural time-histories as corresponding to the underwater and in-air explosions are put into evidence. The effects of the transverse core compressibility on dynamic response are highlighted. In this sense, one of its major implications is the possibility to capture interactively the global and local (wrinkling) dynamic response of the panel. It is shown that implementation of the structural tailoring technique in the face sheets can constitute an important mechanism for enhancing the dynamic load-carrying capacity of sandwich panels when exposed to blast pulses. Effects of the core, the composite architecture of face sheets, orthotropy of the material of the core, geometrical nonlinearities, initial geometric imperfection, and the damping ratio are investigated, and their implications for the dynamic response are highlighted. The comprehensive structural model considered in conjunction with the time-dependent loads generated by the underwater and in-air explosions, and the results obtained in this context, are expected to contribute to a better understanding of the response behavior and to be instrumental toward a better design of these structures.

1. Introduction

SANDWICH CONSTRUCTION has emerged as a most promising type of structure for Navy applications. Its many advantages, including

improved fatigue performance, superior energy absorption that yields an increased resistance to impact, reduced susceptibility to corrosion, superior thermal and acoustic insulation, have generated an increased interest in the extensive incorporation of sandwich composites in the construction of naval structures.

This trend was outlined in the extensive review paper by Mouritz et al. (2001), as well as in the works of the recent inter-

Manuscript received at SNAME headquarters December 15, 2005; revised manuscript received November 18, 2006.

national conferences on sandwich constructions (see the proceedings edited by Vinson et al. 2003 and Thomsen et al. 2005), where some of the achievements in this area have been presented and the potential benefits of the incorporation of sandwich composites in the construction of a variety of naval vessels, including the military ones, have been discussed.

In modern warfare, ships can be exposed to blasts generated by underwater and in-air explosions that can inflict significant damage to their structure. The same is valid when these are exposed during their missions to sonic boom and shock waves.

The possibility of predicting the response of sandwich structural systems to such explosive pulses, without recourse to direct experiments, is of fundamental interest.

Having in view that the structure should withstand the rigors of the blast environment, in order to achieve a reliable design, advanced analytical models of sandwich structures and proper expressions for the blast pulses, generated either by underwater explosions (UNDEX) or in-air explosions (INEX), are needed.

The same is valid for the pressure pulses induced by the sonic boom and shock waves.

In contrast to the case of the homogeneous or standard laminated composite structures, where the effects of transverse normal compressibility can be ignored, for sandwich type constructions this effect can be essential. Indeed, as was shown quite recently (see Hohe and Librescu 2003, 2004a, 2004b), by including the effect of the core compressibility in the modeling of sandwich structures, one can capture both the global and the local (wrinkling) dynamic responses. Moreover, as was shown in previous studies (see, e.g., Frostig et al. 1992) the global and local responses are not independent phenomena, but interdependent ones.

The problems of the global and wrinkling response in the context of the dynamic response of flat sandwich panels to UNDEX and INEX are analyzed in this work.

It should be stressed that in a previous paper (Librescu et al. 2004) the dynamic response problem to UNDEX and INEX was addressed in the context of a less refined structural model (see Librescu et al. 1997b), in the sense of discarding core compressibility in the transverse normal direction, and as a result the possibility of capturing the global and wrinkling dynamic responses was precluded.

In the context of the incorporation of sandwich structures in naval ship constructions and toward their better design, as one of the necessary requirements, a good understanding of the effects of blasts generated by the underwater and in-air explosions and of structural features of sandwich panels on their dynamic response should be reached.

A complexity associated with this issue arises from the fact that the determination of the pressure time-history induced by underwater explosion acting on a sandwich panel involves a more complex analysis than in the case of their monolithic or laminated panel counterparts.

The issue of the dynamic response of sandwich flat panels to time-dependent loads generated by underwater (see Fig. 1) and in-air explosions will be considered in the next developments. In the former case, one supposes that we deal with a submerged panel, whereas in the latter one, with a topside sandwich panel of ship superstructures. In this context, in order to put into evidence the implications of various nonclassical effects, such as those of geometrical nonlinearities, initial geometric imperfections, anisotropy of face sheets and their ply sequence, transverse shear or-

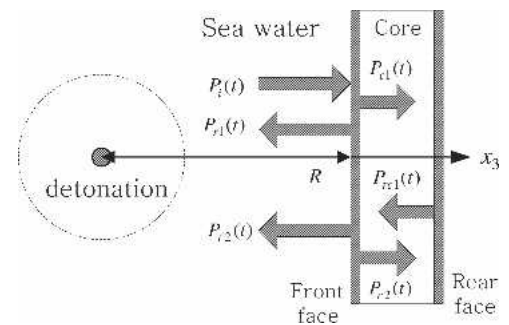


Fig. 1 Sandwich panel subjected to underwater explosion (Reprinted from Librescu, L., Oh, S.-Y., Hohe, J., 2005, Dynamic response of anisotropic sandwich panels to underwater and in-air explosions, in Thomsen, O. T., Bozhevolnaya, E., Lyckegaard, A., editors, *Sandwich Structures 7: Advancing with Sandwich Structures and Materials, Proceedings of the 7th International Conference on Sandwich Structures*, Springer-Verlag, Dordrecht, with kind permission of Springer Science and Business Media.)

thotropy properties of the core layer, and so forth, an advanced model of sandwich constructions will be used. For the more general case of shells, their basic equations have been derived in a number of previous papers (Hohe & Librescu 2003, 2004a, 2004b, Hohe et al. 2006).

However, in order to be self-contained, the basic equations specialized for the case of flat panels that are needed in the treatment and understanding of the subject of this paper are supplied without derivation in Appendix A. Their full derivation was addressed in the previously mentioned papers by Hohe and Librescu.

To the best of the authors' knowledge, with the exception of the works by Hayman (1995), Mäkinen (1999), and Librescu et al. (2004), where special issues on the dynamic response of sandwich panels to underwater explosions have been explored, and of that by Xue and Hutchinson (2003), no other studies on this topic are available in the specialized literature.

2. The structural model: basic assumptions

The global mid-plane of the sandwich flat structure is selected to coincide with that of the core layer. Its points are referred to a curvilinear and orthogonal coordinate system x_a ($a = 1, 2$). The through-the-thickness coordinate x_3 is considered positive when measured in the direction of the downward normal (see Fig. 2). For the sake of convenience, the quantities affiliated with the core layer are identified by the superscript c , while those associated with the face sheets are identified by superscript f .

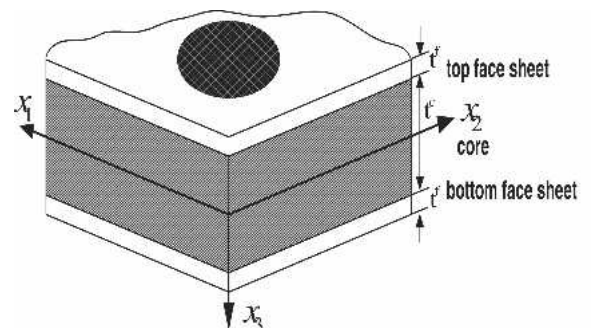


Fig. 2 Geometry of sandwich flat panels with laminated face sheets

The sandwich structural model considered in this paper is based on the following assumptions: (1) the face sheets are composed of a number of orthotropic material laminae, the axes of orthotropy of the individual plies being rotated with respect to the geometrical axes x_{α} of the structure, (2) the material of the core features transverse orthotropic properties, the axes of orthotropy being parallel to the geometrical axes x_{α} , (3) the core layer is capable of carrying transverse shear stresses only, and as a result we deal with a *weak core*. Moreover, one assumes that it is extensible in the transverse normal direction, a feature that will enable the capture of both the global and local (wrinkling) responses, (4) a perfect bonding between the face sheets and the core and between the constituent laminae of the face sheets is assumed to exist, (5) the layers constituting the faces are assumed to be thin; as a result, transverse shear effects are neglected in the face sheets, (6) the structure as a whole, as well as both the top and bottom laminated face sheets, are assumed to exhibit mechanical and geometrical symmetry properties with respect to both the mid-plane of the core layer and about their own mid-planes, as well, and finally, (7) a Lagrangian description of the nonlinear model of sandwich structures is adopted in conjunction with the implementation of the von-Kármán nonlinear kinematic model and of initial geometric imperfections. This feature will enable one to determine the nonlinear dynamic response of the panel.

3. Kinematics

Based on the previously stated assumptions, the basic kinematic relationships derived by Hohe and Librescu (2003, 2004a, 2004b) are supplied next.

The three-dimensional displacement field is represented in terms of two-dimensional displacement measures, in the top and bottom face sheets.

$$v_{\alpha}^t(x_{\alpha}, x_3, t) = u_{\alpha}^t + u_{\alpha}^d - \left(x_3 + \frac{1}{2}(t^c + t^f) \right) u_{3,\alpha}^a - \left(x_3 + \frac{1}{2}(t^c + t^f) \right) u_{3,\alpha}^d, \quad (1)$$

$$v_3^t(x_{\alpha}, x_3, t) = u_3^{\alpha} + u_3^d, \quad (2)$$

$$v_{\alpha}^b(x_{\alpha}, x_3, t) = u_{\alpha}^a - u_{\alpha}^d - \left(x_3 - \frac{1}{2}(t^c + t^f) \right) u_{3,\alpha}^a + \left(x_3 - \frac{1}{2}(t^c + t^f) \right) u_{3,\alpha}^d, \quad (3)$$

$$v_3^b(x_{\alpha}, x_3, t) = u_3^{\alpha} - u_3^d. \quad (4)$$

In these equations, the Greek indices have the range 1, 2, while the Latin indices have the range 1, 2, 3, and unless otherwise stated, Einstein's summation convention over the repeated indices is employed. In addition, $(\cdot)_i$ denotes partial differentiation with respect to coordinate x_i ; superscripts t and b indicate the affiliation of the respective quantities to be top and bottom face sheets, respectively; and t^c and t^f denote the thickness of the core and of face sheets, respectively. Moreover, in the previously displayed equations, there were involved the two-dimensional tangential modified displacement measures represented by the two-dimensional average in-plane displacements and half difference of in-plane displacements, respectively, defined as

$$u_i^a(x_{\alpha}, t) = \frac{1}{2}(u_i^t + u_i^b), \quad u_i^d(x_{\alpha}, t) = \frac{1}{2}(u_i^t - u_i^b), \quad (5)$$

where u_i^t and u_i^b denote the displacements of the points of the mid-planes of the top and bottom face sheets, respectively.

For the core displacement field, a second-order power series expansion of the three-dimensional displacement field is considered:

$$v_{\alpha}^c(x_{\alpha}, x_3, t) = u_{\alpha}^c = \frac{t^f}{2} u_{\alpha}^d + \frac{t^f}{t^c} x_3 u_{3,\alpha}^a + \left(\frac{4(x_3)^2}{(t^c)^2} - 1 \right) \Omega_{\alpha}^c, \quad (6)$$

$$v_3^c(x_{\alpha}, x_3, t) = u_3^a - \frac{2x_3}{t^c} u_3^d \quad (7)$$

where the displacement functions Ω_{α}^c describe the warping of the core. It should be remarked that displacement representations (1) through (7) fulfill identically the kinematic continuity conditions between the face sheets and the core.

The strains of the three constituent structural entities, that is, of bottom and top face sheets and of the core layer, are obtainable from the Lagrangian strain-displacement relations used in conjunction with the von Kármán assumption, namely,

$$2\gamma_{ij} = v_{i,j} + v_{j,i} + v_{3,i}v_{3,j} + \mathring{v}_{3,i}v_{3,j} + v_{3,i}\mathring{v}_{3,j}, \quad (8)$$

where \mathring{v}_3 is the stress-free initial geometric imperfection.

In expanded form, the components of the Green-Lagrange strain tensor are given by:

$$\gamma_{11} = v_{1,1} - \frac{1}{r_1} v_3 + \frac{1}{2}(v_{3,1})^2 + v_{3,1}\mathring{v}_{3,1}, \quad (9)$$

$$\gamma_{22} = v_{2,2} - \frac{1}{r_2} v_3 + \frac{1}{2}(v_{3,2})^2 + v_{3,2}\mathring{v}_{3,2}, \quad (10)$$

$$\gamma_{33} = v_{3,3} + \frac{1}{2}(v_{3,3})^2 + v_{3,3}\mathring{v}_{3,3}, \quad (11)$$

$$\gamma_{23} = \frac{1}{2}(v_{2,3} + v_{3,2}) + \frac{1}{2}v_{3,2}v_{3,3} + \frac{1}{2}v_{3,2}\mathring{v}_{3,3} + \frac{1}{2}\mathring{v}_{3,2}v_{3,3}, \quad (12)$$

$$\gamma_{13} = \frac{1}{2}(v_{1,3} + v_{3,1}) + \frac{1}{2}v_{3,1}v_{3,3} + \frac{1}{2}v_{3,1}\mathring{v}_{3,3} + \frac{1}{2}\mathring{v}_{3,1}v_{3,3}, \quad (13)$$

$$\gamma_{12} = \frac{1}{2}(v_{1,2} + v_{2,1}) + \frac{1}{2}v_{3,1}v_{3,2} + \frac{1}{2}v_{3,1}\mathring{v}_{3,2} + \frac{1}{2}\mathring{v}_{3,1}v_{3,2}, \quad (14)$$

Consistent with the displacement representations, equations (1) to (7), the associated equations of motion and boundary conditions are derived from Hamilton's principle. While these equations are supplied in Appendix A, full details regarding their deduction can be found in the previously indicated papers by Hohe and Librescu (2003, 2004a, 2004b) and Hohe et al. (2006).

4. Blast loads induced by underwater and in-air explosions

Due to the presence of the core layer, the transmission of pressure waves through the sandwich panel renders the problem of determination of the resultant unsteady pressure more intricate than in the case of the monolithic/laminated panel counterparts. In

the latter case, the theory on which the determination of the pressure time-history on the front face of the panel is based follows the line established by Kirkwood-Bethe-Cole. In the former case, the ideas developed specifically for the case of sandwich panels by Hayman (1995), and used subsequently by Mäkinen (1999), will be adopted here.

As will be seen later, the pressure time-histories based on the previously mentioned structural models feature significant quantitative and qualitative differences that affect the dynamic response of the panel in question. Basically, the unsteady pressure model by Hayman (1995) represents an extension for the case of sandwich panels, of that devised for a homogeneous structure by Cole (1948), in the sense of the inclusion also of the pressure transmitted through the core, reflected at the rear face of the sandwich panel and then transmitted out into the water.

Having in view the large blast wave front generated by the explosion, and some conclusions based on the experimental evidence (see, e.g., Houlston et al. 1985), we will adopt the assumption that the resulting pressure over the plate is uniformly distributed.

As a result, the total pressure in front of the sandwich panel can be represented in the following form:

$$P(t) = P_i(t) + P_{r1}(t) + P_{r2}(t), \quad (15)$$

where $P_i(t)$ stands for the free-field pressure due to the incident shock wave; $P_{r1}(t)$ denotes the pressure reflected in the front face, while $P_{r2}(t)$ is the pressure transmitted into the core, reflected at the rear face and transmitted out into the water.

Their expressions are, respectively, as follows:

$$P_i(t) = q_m e^{-(t-t_1)/\Theta}, \quad t \geq t_1 \quad (16)$$

where q_m denotes the peak magnitude of the pressure in the shock front; $t - t_1$ is the time elapsed after the arrival of the shock wave at the panel front surface, where $t_1 = R/c$, c denoting the speed of sound in the sea water, while R is the stand-off distance; Θ is a constant that describes the exponential decay.

For any type of explosive, q_m and Θ are expressed in generic form in terms of the Q (\equiv explosive weight [kg]) and R (\equiv the stand-off distance [m]), as:

$$\begin{aligned} q_m &= K_1(Q^{1/3}/R)^{A_1}, & (\text{MPa}) \\ \Theta &= K_2 Q^{1/3}(Q^{1/3}/R)^{A_2}. & (\text{msec}) \end{aligned} \quad (17a,b)$$

As a result, for any specific explosive, constants K_1 and K_2 and A_1 and A_2 have to be specified correspondingly (see Shin & Geers 1994, Mäkinen 1999). The remaining terms in equation (15) are expressed as

$$P_{r1}(t) = B_1 e^{-\alpha t} + B_2 e^{-\beta t}, \quad (18)$$

$$\begin{aligned} P_{r2}(t) &= E_1 e^{-\alpha(t-t^f/c_c)} + [E_2 + (t - t^f/c_c)E_3] e^{-\beta(t-t^f/c_c)} \\ &+ E_4 e^{-\gamma(t-t^f/c_c)}. \end{aligned} \quad (19)$$

The expressions of the constants appearing in equation (18) are provided next:

$$\alpha = 1/\Theta; \quad \beta = (\rho c + \rho_c c_c)/m_f; \quad \gamma = \rho_c c_c/m_f, \quad (20)$$

where ρ and c are the mass density and speed of sound in the water, respectively, while m_f is the mass of the front face sheet per unit area, c_c ($\equiv \sqrt{E_c/\rho_c}$) denotes the speed of sound in the core,

where E_c and ρ_c are the Young's modulus and mass density of the core material. In addition,

$$\begin{aligned} B_2 &= \frac{2(\beta - \gamma)q_m}{(\beta - \alpha)}; \quad B_1 = q_m - B_2, \\ D_1 &= -\frac{2\gamma(\alpha + \gamma)q_m}{(\beta - \alpha)(\gamma - \alpha)}; \quad D_2 = -\frac{2\gamma(B + \gamma)q_m}{(\beta - \alpha)(\beta - \gamma)}, \\ D_3 &= -(D_1 + D_2), \\ E_1 &= \frac{2(\beta - \gamma)D_1}{(\beta - \alpha)}; \quad E_4 = 2D_3; \quad E_2 = -(E_1 + E_4), \\ E_3 &= 2(\beta - \gamma)D_2. \end{aligned} \quad (21)$$

The above equations that define the expression of the unsteady pressure are applicable to both underwater and in-air explosions. However, in the former case the speed velocity and mass density of the sea water at 20 deg C are $c = 1,476$ m/sec, $\rho = 1,009$ kg/m³, while for the in-air explosion $c = 330$ m/sec and $\rho = 1.20$ kg/m³.

As will be revealed later, this brings in the two investigated cases of underwater and in-air explosions, both qualitative and quantitative considerable differences on the pressure and structural dynamic response.

The supplied pressure expression is not applicable in the case of contact explosion, that is, when the target is located in the immediate proximity of the explosive charge.

In the simulations related to the dynamic response to INEX, we are also considering the cases of the sandwich panel impacted by a sonic boom and an explosive blast. In a compact form, their time-history pressure expressions are (see Marzocca et al. 2001):

$$P(t) = q_m(1 - t/t_p)[H(t) - \delta_b H(t - rt_p)]. \quad (22)$$

In (22), $H(t)$ denotes the Heaviside step function; δ_b is a tracer that takes the values 1 or 0 depending on whether the sonic boom or the triangular blast is considered, respectively; t_p denotes the positive phase duration of the pulse measured from the time of impact of the structure; r denotes the shock pulse length factor, while q_m is the pressure in excess of the ambient one. For $r = 1$, the sonic boom reduces to a triangular explosive pulse, while for $r = 2$ it corresponds to a symmetric sonic boom pulse.

In connection with the expressions provided by equation (22), note that (1) the pressure corresponding to the explosive blast (i.e., for $\delta_b = 0$) constitutes a special case of the Friedlander exponential decay blast equation obtained in the context of modeling of shock waves in a compressible gas, and of that obtainable from the previously supplied equations, while (2) the sonic boom pressure signature obtained for $\delta_b = 1$ that corresponds to an N -wave shock pulse impacting the structure at a normal incidence was obtained by considering the shock wave in a supersonic gas flow. For a review of its analytical approach, the reader is referred to Gottlieb and Ritzel (1988).

Within the INEX problem, we will consider also the case of the tangential blast to the panel surface in the direction of the coordinate x_1 in the form of a traveling wave:

$$P(t) = q_m H(ct - x_1) \exp[-\eta(ct - x_1)], \quad (23)$$

where c is the wave speed in the medium surrounding the structure, while η is an exponent characterizing the blast decay. As

Table 1 Elastic coefficients for the materials of face sheets and core layers

Face sheets	
E_1 (GPa)	207
E_2 (GPa)	5.17
G_{12} (GPa)	2.55
ν_{12}	0.25
ρ_f (kg/m ³)	1,588.22
Core layer	
G_{13} (GPa)	0.1027
G_{23} (GPa)	0.0621
ρ_c (kg/m ³)	16

shown by Vol'mir (1976), this expression provides excellent agreements of the response time-histories with those obtained by experimental means.

5. Results

Selected results on the dynamic response of square $l_1 = l_2 \equiv L$ sandwich panels of the total thickness $t^c + t^f = H$ to UNDEX and INDEX are presented next. The numerical results presented here have considered the case of face sheets laminated from the same orthotropic material, whose axes of orthotropy are rotated with respect to the geometrical axes of the panel by an angle θ . For the face sheets, a material characterized by a rather large in-plane orthotropicity ratio was considered. Its properties, as well as those of the core layer, are given in Table 1.

In all numerical simulations, the geometrically nonlinear structural model was used, and unless otherwise stated, the stacking sequence of face sheets is as follows: [0/90 deg/0/90 deg/0/core/0/90 deg/0/90 deg/0].

The sandwich rectangular panel is assumed to be simply supported all over the contour, the edges being unloaded and immov-

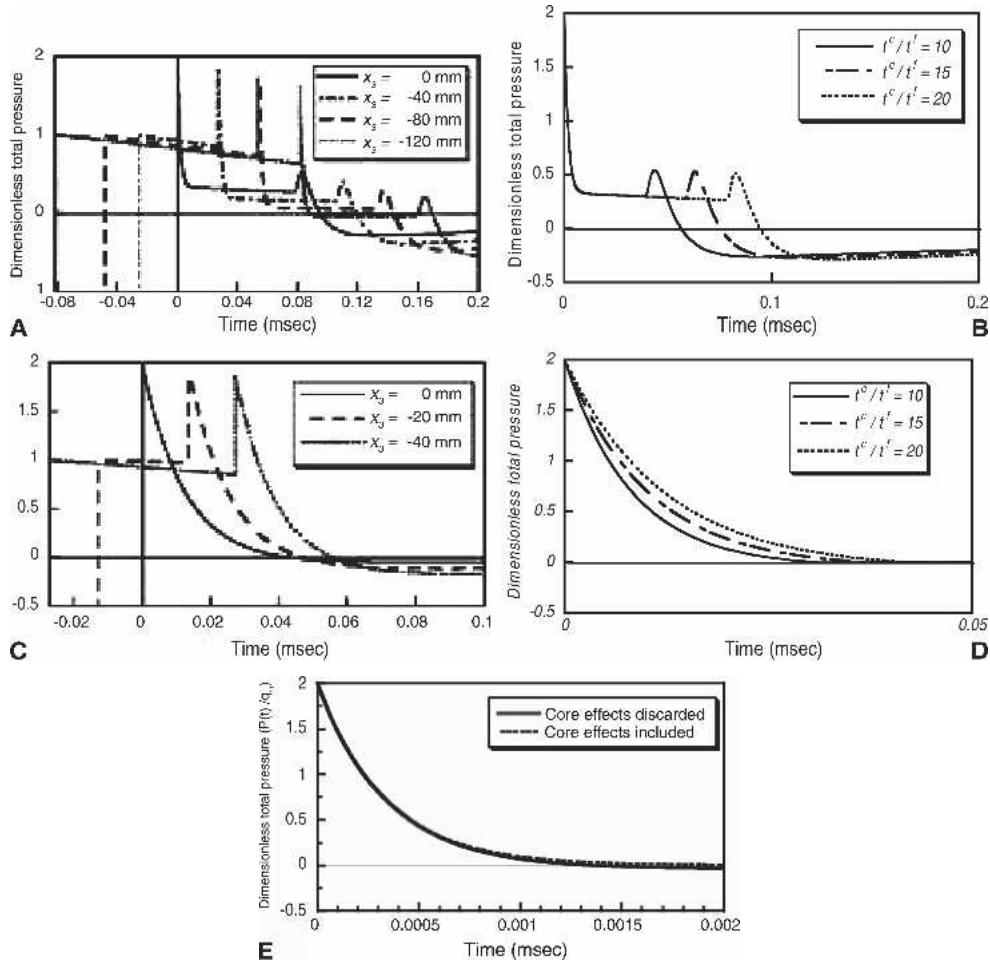


Fig. 3 (a) Dimensionless pressure time-history, $P(t)/q_m$, for various distances from panel front surface in UNDEX. Effect of the pressure transmission through the core included. ($Q = 30$ Kg, $R = 10$ m, $\rho_f/\rho_c = 5$, $t^c/t^f = 20$, $L/H = 15$). (b) Influence of the thickness ratio t_c/t_f on dimensionless pressure time-history, $P(t)/q_m$, in UNDEX on the front face of the panel. Effect of pressure transmission through the core included. The remaining data are as in panel a. (c) The counterpart of panel a when the compressibility of the core is discarded. (d) Influence of the thickness ratio on dimensionless pressure time-history, $P(t)/q_m$, in UNDEX. Effect of pressure transmission through the core is discarded ($Q = 30$ Kg, $R = 10$ m, $x_3 = 0$, $\rho_f = 15.28$ Kg/m³). (e) Dimensionless pressure time-histories, $P(t)/q_m$, at the panel surface in INEX ($Q = 30$ Kg, $R = 10$ m, $\rho_f/\rho_c = 5$, $t^c/t^f = 20$). (Reprinted from Librescu, L., Oh, S.-Y., Hohe, J., 2005, Dynamic response of anisotropic sandwich panels to underwater and in-air explosions, in Thomsen, O. T., Bozhevolnaya, E., Lyckegaard, A., editors, *Sandwich Structures 7: Advancing with Sandwich Structures and Materials, Proceedings of the 7th International Conference on Sandwich Structures*, Springer-Verlag, Dordrecht, with kind permission of Springer Science and Business Media.)

able in the tangential direction, normal to the panel edge. In this case, compressive edge forces induced by the edge immovability will be generated.

The equations displayed in the Appendix reveal a full coupling between the global and local (wrinkling) motions. The number of eight boundary conditions prescribed at each edge indicates that the order of the governing equation system should be sixteen.

From the mathematical point of view the problem at hand, namely, that of the dynamic response, reduces to the solution of a dynamic nonlinear boundary value problem.

Due to the intricacy of the present boundary value problem, an approximate solution methodology based on the extended Galerkin method (EGM) coupled with the satisfaction of the tangential boundary conditions on an average sense was used. This methodology was presented in detail in the papers by Hause et al. (1998) and Librescu et al. (2000), in a more general context in Librescu et al. (1997) and Librescu and Song (2005), and will not be repeated here.

It should be stressed that the predictions provided by the application of the EGM are of an extreme accuracy, these being identical in many instances to the exact ones. In this sense, the reader is referred to Song et al. (1998) where, in the context of a linearized boundary-value problem, a perfect agreement of predictions on dynamic response obtained via EGM and the Laplace transform method was reported.

The results supplied in Fig. 3, *a* and *b*, correspond to the pressure time-history induced by an UNDEX at various distances from the front face of a sandwich panel. In both figures the effects of the transmission of pressure waves through the core have been included.

In contrast, in Fig. 3, *c* and *d*, the counterparts of Fig. 3, *a* and *b*, for the case of the discard of the core compressibility effects are presented.

From these figures, qualitative and quantitative differences are emerging. First of all, one can observe that in the case of the inclusion of the core effects, the time at which the cavitation occurs (i.e., the time corresponding to the instant when the resultant pressure becomes a zero-valued quantity) is much larger than that corresponding to the discard of core effects. In addition, in the former case, almost two simultaneous cavitation events occur, one on the front face of the sandwich panel and the second one at a small distance in front of it. In the latter case, a single cavitation takes place. These results are in excellent agreement with those reported by Hayman (1995) and Mäkinen (1999).

It is also interesting to see the pressure time-history due to an INEX when the core effects are included or discarded.

In this sense, Fig. 3*e* reveals, on the one hand, that the in-air explosion is much more severe than in the water, and on the other hand, that the transmission of the pressure wave through the core and its reflection on the rear face bring, in this case, no changes as compared to the case of the discard of this effect.

In Fig. 4*a* the global deflection time-history of the sandwich panel as influenced by the structural damping and by incorporation/discard of the face wrinkling is depicted. It clearly appears that the effect of the wrinkling on the global response is immaterial.

In Fig. 4*b*, the dimensionless wrinkling displacement time-history for the case of two values of the damping parameter is presented.

The results reveal that the face wrinkling, the occurrence of which should be contained at any price, is very sensitive to the structural damping, in the sense that even for $\zeta (= C/2m_0\omega_1) = 0.02$, the face wrinkling oscillation will damp out after a very short

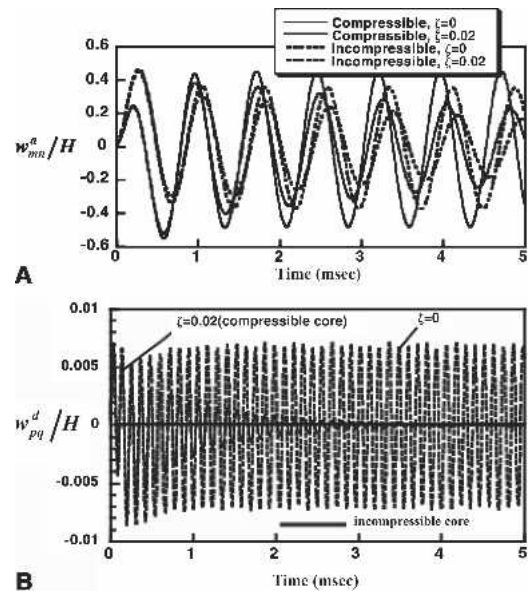


Fig. 4 (a) The global dimensionless transverse deflection time-history ($Q = 30$ Kg, $R = 10$ m, $\dot{w}_{mn}^a = 0.1$ H, $\dot{w}_{pq}^d = 0.01$ H). (b) Dimensionless face wrinkling deflection time-history of the panel subjected to UNDEX ($Q = 30$ Kg, $R = 10$ m, $\dot{w}_{mn}^a = 0.1$ H, $\dot{w}_{pq}^d = 0.01$ H). (Reprinted from Librescu, L., Oh, S.-Y., Hohe, J., 2005, Dynamic response of anisotropic sandwich panels to underwater and in-air explosions, in Thomsen, O. T., Bozhevolnaya, E., Lyckegaard, A., editors, *Sandwich Structures 7: Advancing with Sandwich Structures and Materials, Proceedings of the 7th International Conference on Sandwich Structures*, Springer-Verlag, Dordrecht, with kind permission of Springer Science and Business Media.)

time. In the expression of the damping parameters, ω_1 is the undamped fundamental natural frequency of the structure.

In Fig. 5*a*, results emerging from the implementation of the tailoring technique in the face sheets on the global deflection time-history are presented. The results reveal that a notable reduction of the oscillation amplitude is obtained by a proper selection of the ply angle in the face sheets.

However, as revealed in Fig. 5*b*, for the wrinkling deflection time-history, implementation of the tailoring technique appears to be less efficient than in the case of the global response.

As concerns the effect of the increase of the transverse Young's modulus in the core layer on the global and wrinkling response, Fig. 6, *a* and *b*, reveals that the increase is strongly beneficial in the case of the wrinkling displacement, and it appears to be rather weak in the case of the global response.

Fig. 7, *a* and *b*, shows the effects of the stand-off and weight charge, respectively, on the velocity and acceleration time-history of the center of the panel subjected to an underwater explosion. The values of the velocity response in UNDEX as presented here are in agreement with those reported by Jiang and Olsen (1994).

The considerable increase of the severity of the in-air explosion (these results are not supplied here) as compared to that in the underwater explosion should be noticed.

The dynamic response, global and local (wrinkling), to a sonic boom pulse and, in this sense, the effects of the pulse increase measured in terms of the parameter r are presented in Fig. 8, *a* and *b*, respectively.

The results reveal that the asymmetric ($r = 1.2$) sonic boom is

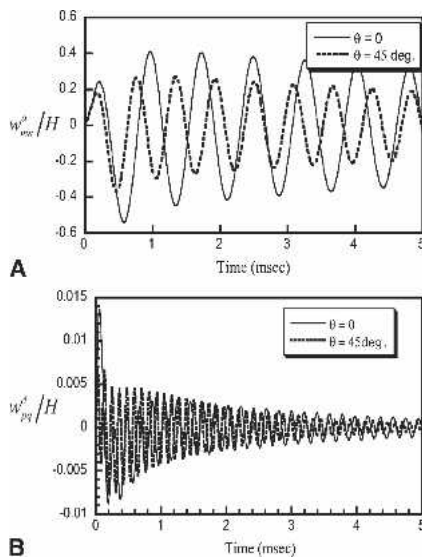


Fig. 5 (a) Effect of the ply angles of faces on the global transverse deflection time-history ($Q = 30$ Kg, $R = 5$ m, $\dot{w}_{mn}^a = 0.1$ H, $\dot{w}_{pq}^d = 0.01$ H, $G_{13} = 11 \times 10^6$ Pa, $G_{23} = 2G_{13}$, $\zeta = 0.01$). (b) Effect of the ply angle of face sheets on the wrinkling deflection time-history ($Q = 30$ Kg, $R = 5$ m, $\dot{w}_{mn}^a = 0.1$ H, $\dot{w}_{pq}^d = 0.01$ H, $G_{13} = 11 \times 10^6$ Pa, $G_{23} = 2G_{13}$) UNDEX. (Reprinted from Librescu, L., Oh, S.-Y., Hohe, J., 2005, Dynamic response of anisotropic sandwich panels to underwater and in-air explosions, in Thomsen, O. T., Bozhevolnaya, E., Lyckegaard, A., editors, *Sandwich Structures 7: Advancing with Sandwich Structures and Materials, Proceedings of the 7th International Conference on Sandwich Structures*, Springer-Verlag, Dordrecht, with kind permission of Springer Science and Business Media.)

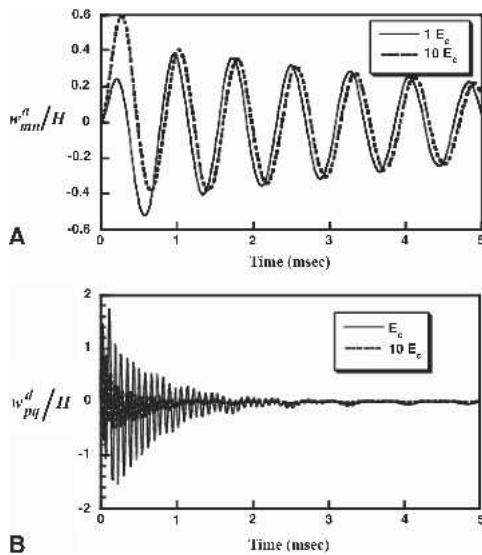


Fig. 6 (a) The effect of the transverse Young's modulus of the core on the overall transverse deflection time-history of the panel subjected to UNDEX ($Q = 30$ Kg, $R = 5$ m, $\dot{w}_{mn}^a = 0.1$ H, $\dot{w}_{pq}^d = 0.01$ H, $E_3 = 30 \times 10^6$ Pa, $\zeta = 0.02$). (b) The counterpart of panel a for the wrinkling dynamic response. (Reprinted from Librescu, L., Oh, S.-Y., Hohe, J., 2005, Dynamic response of anisotropic sandwich panels to underwater and in-air explosions, in Thomsen, O. T., Bozhevolnaya, E., Lyckegaard, A., editors, *Sandwich Structures 7: Advancing with Sandwich Structures and Materials, Proceedings of the 7th International Conference on Sandwich Structures*, Springer-Verlag, Dordrecht, with kind permission of Springer Science and Business Media.)

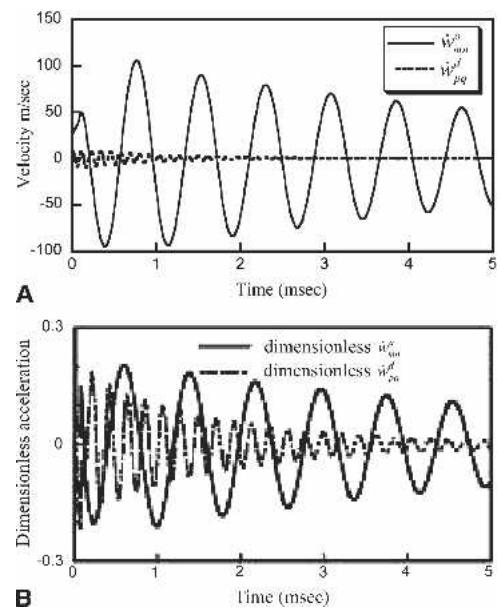


Fig. 7 (a) Velocity time-history on global and face wrinkling of the panel subjected to underwater explosion ($Q = 30$ Kg, $R = 5$ m, $\dot{w}_{mn}^a = 0.1$ H, $\dot{w}_{pq}^d = 0.01$ H, $\zeta = 0.02$). (b) Dimensionless acceleration time-history on global and face wrinkling of the center panel subjected to UNDEX. The data are as in panel a. (Reprinted from Librescu, L., Oh, S.-Y., Hohe, J., 2005, Dynamic response of anisotropic sandwich panels to underwater and in-air explosions, in Thomsen, O. T., Bozhevolnaya, E., Lyckegaard, A., editors, *Sandwich Structures 7: Advancing with Sandwich Structures and Materials, Proceedings of the 7th International Conference on Sandwich Structures*, Springer-Verlag, Dordrecht, with kind permission of Springer Science and Business Media.)

more severe than the symmetric ($r = 1$) one. As a special case, the results reveal that the effects of the sonic boom are more severe than those due to a triangular blast.

In Fig. 9, *a* and *b*, the effects of face sheet ply angle on both the global and wrinkling response to a sonic boom are presented, respectively. In this case, the following architecture of the sandwich structure was considered, namely: $[\theta/-\theta/\theta/-\theta/\theta]$ core $[\theta/-\theta/\theta/-\theta/\theta]$. The results show that the tailoring of face sheets can have a strong beneficial effect, especially on the wrinkling response and less on the global response.

Figure 10, *a* and *b*, highlights the effects of the peak pressure on global and wrinkling dynamic response, respectively, of the panel mid-point when exposed to a sonic boom pulse. The results reveal that while q_m has an important effect on the global response, its influence on the local one appears to be rather marginal.

Finally, the dynamic response of the sandwich panel exposed to an in-air tangential blast, the pressure expression of which is provided by equation (23), is highlighted in Figs. 11 (*a*, *b*) and 12 (*a*, *b*) where, for selected values of η and c , the global and local (wrinkling) time-history deflections of the panel center are depicted.

It is shown that the increases of the blast decay η and of wave speed parameter c yield a stronger decay of the wrinkling deflection amplitude than of the global one.

6. Conclusions

The problem of the dynamic response of sandwich flat panels subjected to explosive blast loadings produced by both underwater

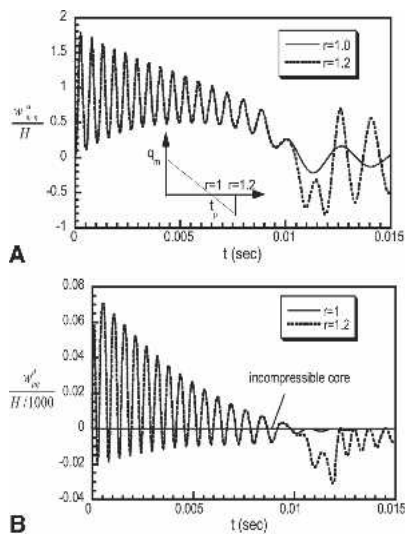


Fig. 8 (a) Effect of sonic boom pulse on the global dynamic response of a flat sandwich panel ($\zeta = 0.1$, $\dot{w}_{mn}^a = 0.01 H$, $\dot{w}_{pq}^d = 0.0001 H$, $L/H = 15$, $t_p = 0.01$ sec, $q_m = 10$ MPa). (b) Counterpart of panel a for the wrinkling dynamic response. (Reprinted from Librescu, L., Oh, S.-Y., Hohe, J., 2005, Dynamic response of anisotropic sandwich panels to underwater and in-air explosions, in Thomsen, O. T., Bozhevolnaya, E., Lyckegaard, A., editors, *Sandwich Structures 7: Advancing with Sandwich Structures and Materials, Proceedings of the 7th International Conference on Sandwich Structures*, Springer-Verlag, Dordrecht, with kind permission of Springer Science and Business Media.)

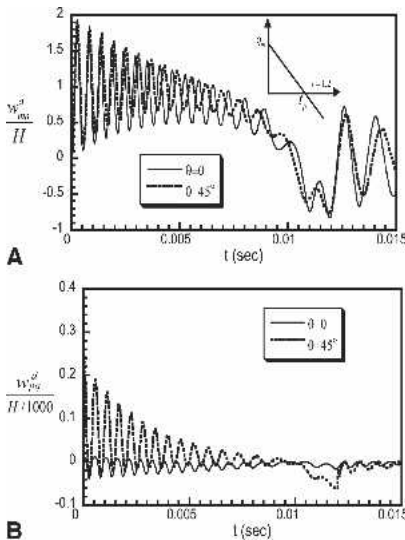


Fig. 9 (a) Effect of ply angle of face sheets on the global instability of the sandwich panel ($\zeta = 0.1$, $\dot{w}_{mn}^a = 0.1 H$, $\dot{w}_{pq}^d = 0.0001 H$, $q_m = 10$ MPa, $G_{23} = 5G_{13} = 11$ MPa, $t_p = 0.01$ sec, $r = 1.2$). (b) Counterpart of panel a for the wrinkling response of the sandwich panel. (Reprinted from Librescu, L., Oh, S.-Y., Hohe, J., 2005, Dynamic response of anisotropic sandwich panels to underwater and in-air explosions, in Thomsen, O. T., Bozhevolnaya, E., Lyckegaard, A., editors, *Sandwich Structures 7: Advancing with Sandwich Structures and Materials, Proceedings of the 7th International Conference on Sandwich Structures*, Springer-Verlag, Dordrecht, with kind permission of Springer Science and Business Media.)

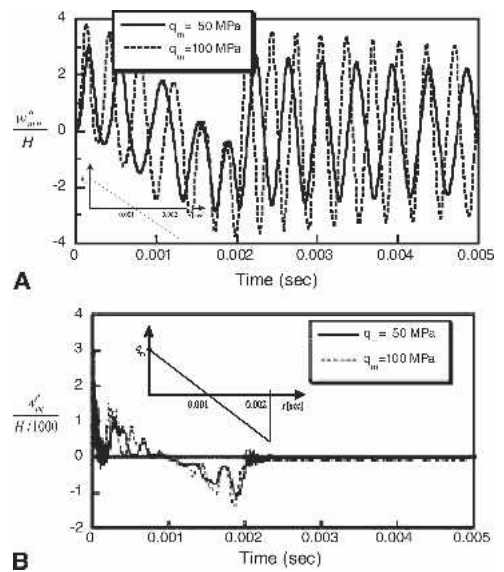


Fig. 10 (a) Effect of the peak pressure generated by a sonic boom on the global response $\zeta = 0.05$, $\dot{w}_{mn}^a = 0.01 H$, $\dot{w}_{pq}^d = 0.0001$, $L/H = 15$, $r = 2$, $t_p = 0.001$ sec. (b) The counterpart of the case in panel a on the wrinkling response. (Reprinted from Librescu, L., Oh, S.-Y., Hohe, J., 2005, Dynamic response of anisotropic sandwich panels to underwater and in-air explosions, in Thomsen, O. T., Bozhevolnaya, E., Lyckegaard, A., editors, *Sandwich Structures 7: Advancing with Sandwich Structures and Materials, Proceedings of the 7th International Conference on Sandwich Structures*, Springer-Verlag, Dordrecht, with kind permission of Springer Science and Business Media.)

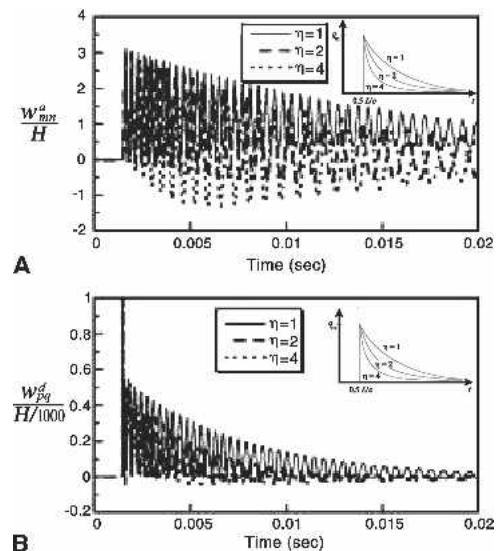


Fig. 11 (a) Effect of the decay parameter η on global response of the center panel subjected to a traveling blast ($\zeta = 0.05$, $\dot{w}_{mn}^a = 0.01 H$, $\dot{w}_{pq}^d = 0.0001 H$, $L/H = 15$, $q_m = 50$ MPa, $c = 150$ m/s). (b) The counterpart of panel a for the local response. (Reprinted from Librescu, L., Oh, S.-Y., Hohe, J., 2005, Dynamic response of anisotropic sandwich panels to underwater and in-air explosions, in Thomsen, O. T., Bozhevolnaya, E., Lyckegaard, A., editors, *Sandwich Structures 7: Advancing with Sandwich Structures and Materials, Proceedings of the 7th International Conference on Sandwich Structures*, Springer-Verlag, Dordrecht, with kind permission of Springer Science and Business Media.)

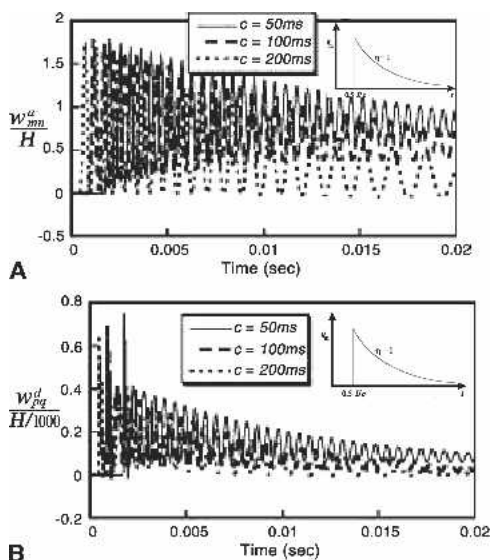


Fig. 12 (a) Effect of the velocity of the traveling blast on global dynamic response of the center panel ($\zeta = 0.05$, $\dot{w}_{mn}^a = 0.01$ H, $\dot{w}_{pq}^d = 0.0001$ H, $L/H = 15$, $\eta = 1$, $q_m = 10$ MPa). (b) The counterpart of panel a for the local response. (Reprinted from Librescu, L., Oh, S.-Y., Hohe, J., 2005, Dynamic response of anisotropic sandwich panels to underwater and in-air explosions, in Thomsen, O. T., Bozhevolnaya, E., Lyckegaard, A., editors, *Sandwich Structures 7: Advancing with Sandwich Structures and Materials*, Proceedings of the 7th International Conference on Sandwich Structures, Springer-Verlag, Dordrecht, with kind permission of Springer Science and Business Media.)

and in-air explosions has been addressed. The implications of a number of structural and geometrical characteristics of the sandwich panel, as well as of the ones related to the respective blasts, have been highlighted and related conclusions have been drawn. Consideration of the compressibility of the core in the cases of the UNDEX and INEX has been shown to result in qualitatively and quantitatively different results, from both the pressure time-history and the structural response points of view.

The obtained results can be extended to determine the time-histories of strain and stress components at various points of the structure. These items are essential for determining the structural failure.

Other issues that are of high relevance in the context of this problem, related to bulk and local cavitations, bubble-pulse loading and bubble behavior, and jetting effects on the dynamic response of submerged sandwich panels exposed to an explosion, have not been addressed here. However, the structural model presented in this paper can constitute a sound basis for the approach of these important problems.

Acknowledgment

The financial support of the Office of Naval Research Program on Composites for Marines Structures, Grant N000014-02-1-0594, and the interest, advice, and encouragement of the Program Manager, Dr. Y. D. S. Rajapakse, are gratefully acknowledged.

References

COLE, R. H. 1948 *Underwater Explosions*, Princeton University Press, Princeton, NJ.

FROSTIG, Y., BARUCH, M., VILNAY, O., AND SHEIMAN, I. 1992 High-order buckling theory for sandwich-beam behavior with transversely flexible core, *Journal of Engineering Mechanics*, **118**, 1026–1043.

GOTTLIEB, J. J., AND RITZEL, D. V. 1988 Analytical study of sonic boom from supersonic projectiles, *Progress in Aerospace Sciences*, **25**, 131–138.

HAUSE, T., LIBRESCU, L., AND CAMARDA, C. J. 1998 Postbuckling of anisotropic flat and doubly-curved sandwich panels under complex loading conditions, *International Journal of Solids and Structures*, **35**, 2007–3028.

HAYMAN, B. 1995 Underwater explosion loading on foam-cored sandwich panels, *Proceedings, 3rd International Conference on Sandwich Construction (EMAS)*, May 11–15, Southampton, England.

HOHE, J., AND LIBRESCU, L. 2003 A nonlinear theory for doubly curved anisotropic sandwich shells with transversely compressible core, *International Journal of Solids and Structures*, **40**, 1059–1088.

HOHE, J., AND LIBRESCU, L. 2004a Core and face sheet anisotropy in deformation and buckling of sandwich panels, *AIAA Journal*, **42**, 149–158.

HOHE, J., AND LIBRESCU, L. 2004b Advances in the structural modeling and behavior of sandwich panels, *Mechanics of Advanced Materials and Structures*, **11**, 395–424.

HOHE, J., LIBRESCU, L., AND OH, S.-Y. 2006 Dynamic buckling of flat and curved sandwich panels with transversely compressible core, *Composite Structures*, **74**, 10–24.

HOULSTON, R., SLATER, J. E., PEGG, N., AND DESROCHERS, C. G. 1985 On analysis of structural response of ship panels subjected to air blast loading, *Computers and Structures*, **21**, 2, 273–289.

JIANG, J., AND OLSEN, M. D. 1994 *Modeling of Underwater Shock-Induced Response of Thin Plate Structures*, Report No. 39, Department of Civil Engineering, University of British Columbia, Vancouver, BC.

LIBRESCU, L., HAUSE, T., AND JOHNSON, T. F. 2000 Buckling and nonlinear response of sandwich curved panels to combined mechanical loads—implications of face-sheets elastic tailoring, *Journal of Sandwich Structures and Materials*, **2**, 246–269.

LIBRESCU, L., OH, S.-Y., AND HOHE, J. 2004 Linear and nonlinear dynamic response of sandwich panels to blast loading, *Composites B, Special Issues on Marine Composites* (Rajapakse, Y. D. S., and Hui, D., editors) **35**, 6–8, 795–803.

LIBRESCU, L., MEIROVITCH, L., AND NA, S. S. 1997a Control of cantilevers vibration via structural tailoring and adaptive materials, *AIAA Journal*, **35**, 8, 1309–1315.

LIBRESCU, L., HAUSE, T., AND CAMARDA, C. J. 1997b Geometrically nonlinear theory of initially imperfect sandwich plates and shells incorporating nonclassical effects, *AIAA Journal*, **35**, 8, 1392–1403.

LIBRESCU, L., AND SONG, O. 2005 *Composite Thin-Walled Beams: Theory and Application*, Springer.

MÄKINEN, K. 1999 *Underwater Shock Loaded Sandwich Structures*, Department of Aeronautics, Royal Institute of Technology, Report 99-01, Stockholm, Sweden.

MARZOCCA, P., LIBRESCU, L., AND CHIOCCHIA, G. 2001 Aeroelastic response of 2-D lifting surfaces to gust and arbitrary explosive loading signature, *International Journal of Impact Engineering*, **25**, 1, 67–85.

MOURITZ, A. P., GELLERT, E., BURCHHILL, P., AND CHALLIS, K. 2001 Review of advanced composite structure for naval ships and submarines, *Composite Structures*, **53**, 21–41.

SHIN, Y. S., AND GEERS, T. L. 1994 *Response of Marine Structures to Underwater Explosions*, International Short Course Notebook, Shock and Vibration Research, Monterey, CA.

SONG, O., JU, J. S., AND LIBRESCU, L. 1998 Dynamic response of anisotropic thin-walled beams to blast and harmonically oscillating loads, *International Journal of Impact Engineering*, **21**, 8, 663–682.

THOMSEN, O. T., BOZHEVOLNAYA, E., AND LYCHEGAARD, A., EDITORS. 2005 *Sandwich Structures 7: Advancing with Sandwich Structures and Materials* (Proceedings of the 7th International Conference on Sandwich Structures, Aalborg, Denmark, August 29–31, 2005), Springer-Verlag, Dordrecht.

VINSON, J. R., RAJAPAKSE, Y. D. S., AND CARLSSON, L. E., editors. 2003 *Sixth International Conference on Sandwich Structures*, CRC Press, Boca Raton, London.

VOL'MIR, A. S. 1976 *Shells in Fluid and Gas Flows—Aeroelasticity Problems* (in Russian), Nauka, Moscow, Russia.

XUE, Z., AND HUTCHINSON, J. W. 2003 Preliminary assessment of sandwich plates subject to blast loads, *International Journal of the Mechanical Sciences*, **45**, 687–705.

Appendix

Equations of motion and boundary conditions

Consistent equations of motion and boundary conditions are derived from Hamilton's principle:

$$\int_{t^0}^{t^1} (\delta U - \delta W - \delta T) dt = 0 \quad (A1)$$

where δU , δW , and δT are the variations of the strain energy, of the work done by the external loads, and of the kinetic energy, respectively, in the case of a virtual displacement δu_i^a and δu_i^d of the sandwich structure during the time interval $[t^0, t^1]$. The variations of the energy components δU , δW , and δT are expressed in terms of the components τ_{ij} of the second Piola-Kirchhoff stress tensor and the variations $\delta \gamma_{ij}$ of the Green-Lagrange strain tensor, which, subsequently, are expressed in terms of the virtual displacement δu_i^a and δu_i^d by virtue of equations (9) through (14), in conjunction with equations (1) through (7). In this context, only transverse distributed loads \hat{q}_3^t and \hat{q}_3^b are considered. In a similar manner, only the transverse inertia effects are considered, whereas the tangential inertia terms are discarded (see Hohe and Librescu 2003 for details).

In the resulting expression, the integrals of the three-dimensional stress components with respect to the transverse (x_3) direction are substituted by the equivalent two-dimensional in-plane and bending stress resultants.

Integrating (A1) by parts wherever feasible, the terms corresponding to the virtual displacement δu_i^a and δu_i^d are collected. Since the virtual displacements are arbitrary and independent from each other, the corresponding coefficients must vanish independently. Thus, the following equations of motion are obtained:

$$N_{\alpha\beta,\beta}^a = 0, \quad (A2)$$

$$N_{\alpha\beta,\beta}^d + N_{\alpha 3}/t^c = 0, \quad (A3)$$

$$\begin{aligned} M_{\alpha\beta,\alpha\beta}^a + (u_{3,\alpha\beta}^a + \hat{u}_{3,\alpha\beta}^a) N_{\alpha\beta}^a + (u_{3,11}^d + \hat{u}_{3,11}^d) N_{11}^d + [(t^c + t^f)/2 \\ - u_3^d - \hat{u}_3^d] N_{\alpha 3,\alpha}^c / t^c - 2(u_{3,\alpha}^d + \hat{u}_{3,\alpha}^d) N_{\alpha 3}^c / h^c + \hat{q}_3^a \\ - (m^f + m^c/2) \hat{u}_3^a - C \hat{u}_3^a = 0, \end{aligned} \quad (A4)$$

$$\begin{aligned} M_{\alpha\beta,\alpha\beta}^d + (u_{3,\alpha\beta}^a + \hat{u}_{3,\alpha\beta}^a) N_{\alpha\beta}^a + (u_{3,\alpha\beta}^d + \hat{u}_{3,\alpha\beta}^d) N_{\alpha\beta}^d \\ + (u_{3,\alpha\beta}^d + \hat{u}_{3,\alpha\beta}^d) N_{\alpha\beta}^a + 2[t^c/2 - u_3^d - \hat{u}_3^d] N_{33}^c / t^c + \hat{q}_3^d \\ - (m^f + m^c/6) \hat{u}_3^d - C \hat{u}_3^d = 0 \end{aligned} \quad (A5)$$

In the previous equations \hat{u}_3^a and \hat{u}_3^d are the prescribed initial geometric imperfections; m^f and m^c are the integrated mass densities of the face sheets and the core, respectively; \hat{q}_3 denotes the prescribed transverse distributed load; and C is the structural damping coefficient.

In equations (A2) through (A5), the modified stress resultants and stress couples similar to the definitions of the average and difference displacement functions u_i^a and u_i^d , equation (5), are used.

$$\{N_{\alpha\beta}^a, M_{\alpha\beta}^a, \hat{q}_3^a\} = \frac{1}{2} \left\{ \begin{array}{l} (N_{\alpha\beta}^t + N_{\alpha\beta}^b), (M_{\alpha\beta}^t + M_{\alpha\beta}^b), \\ (\hat{q}_3^t + \hat{q}_3^b) \end{array} \right\} \quad (A6)$$

$$\{N_{\alpha\beta}^d, M_{\alpha\beta}^d, \hat{q}_3^d\} = \frac{1}{2} \left\{ \begin{array}{l} (N_{\alpha\beta}^t - N_{\alpha\beta}^b), (M_{\alpha\beta}^t - M_{\alpha\beta}^b), \\ (\hat{q}_3^t - \hat{q}_3^b) \end{array} \right\} \quad (A7)$$

These are expressed in terms of the conventional stress resultants and stress couples defined as

$$\{N_{\alpha\beta}^t, M_{\alpha\beta}^t\} = \int_{-h^f - \frac{h^c}{2}}^{-\frac{h^2}{2}} \tau_{\alpha\beta}^t \left\{ 1, \left(x_3 + \frac{h^c + h^f}{2} \right) \right\} dx_3, \quad (A8)$$

$$\{N_{\alpha\beta}^b, M_{\alpha\beta}^b\} = \int_{\frac{h^c}{2}}^{h^f + \frac{h^c}{2}} \tau_{\alpha\beta}^b \left\{ 1, \left(x_3 - \frac{h^c + h^f}{2} \right) \right\} dx_3, \quad (A9)$$

$$\{N_{i3}^c, M_{i3}^c\} = \int_{\frac{h^c}{2}}^{\frac{h^c}{2}} \tau_{i3}^c \{1, x_3\} dx_3. \quad (A10)$$

The corresponding boundary conditions obtained also from Hamilton's principle read

$$\begin{aligned} u_n^a = \hat{u}_n^a \text{ or: } N_{nn}^a = \hat{N}_{nn}^a, \\ u_t^a = \hat{u}_t^a \text{ or: } N_{nt}^a = \hat{N}_{nt}^a, \\ u_n^d = \hat{u}_n^d \text{ or: } N_{nn}^d = \hat{N}_{nn}^d, \\ u_t^d = \hat{u}_t^d \text{ or: } N_{nt}^d = \hat{N}_{nt}^d, \end{aligned} \quad (A11)$$

$$\begin{aligned} u_3^a = \hat{u}_3^a \text{ or: } (u_{3,n}^a + \hat{u}_{3,n}^a) N_{nn}^a + (u_{3,t}^a + \hat{u}_{3,t}^a) N_{nt}^a + (u_{3,n}^d + \hat{u}_{3,n}^d) N_{nn}^d \\ + (u_{3,t}^d + \hat{u}_{3,t}^d) N_{nt}^d + M_{nn,n}^a + 2M_{nt,t}^a + \frac{1}{h^c} \left(\frac{h^c + h^f}{2} - u_3^d - \hat{u}_3^d \right) N_{n3}^c \\ - \hat{M}_{nt,t}^a + \frac{1}{2} \hat{N}_{n3}^c, \end{aligned}$$

$$\begin{aligned} u_3^d = \hat{u}_3^d \text{ or: } (u_{3,n}^a + \hat{u}_{3,n}^a) N_{nn}^d + (u_{3,t}^a + \hat{u}_{3,t}^a) N_{nt}^d + (u_{3,n}^d + \hat{u}_{3,n}^d) N_{nn}^a \\ + (u_{3,t}^d + \hat{u}_{3,t}^d) N_{nt}^a + M_{nn,n}^d + 2M_{nt,t}^d = \hat{M}_{nt,t}^d - \frac{1}{h^c} \hat{M}_{n3}^c, \end{aligned}$$

$$u_{3,n}^a = \hat{u}_{3,n}^a \text{ or: } M_{nn}^a = \hat{M}_{nn}^a,$$

$$u_{3,n}^d = \hat{u}_{3,n}^d \text{ or: } M_{nn}^d = \hat{M}_{nn}^d,$$

where n and t are the normal and tangential directions to the boundary. One should consider $n = 1$, when $t = 2$, and $n = 2$, when $t = 1$. The prescribed quantities on the boundaries are indicated by an overcaret. For homogeneous boundary conditions, these quantities are immaterial.

Orthotropic materials are assumed for both the core and the face sheets. Whereas for the core, the axes of in-plane orthotropy are assumed to coincide with the axes x_i of the local coordinate sys-

tem, for the face sheets, the orthotropy axes are assumed to be rotated with respect to the geometrical ones. Thus, the in-plane and bending face sheet stress resultants $N_{\alpha\beta}^f$ and $M_{\alpha\beta}^f$ are related to the mid-surface and bending strains $\gamma_{\alpha\beta}^f$ and $\kappa_{\alpha\beta}^f$ of the corresponding face sheets by

$$\begin{pmatrix} N_{11}^f \\ N_{22}^f \\ N_{12}^f \end{pmatrix} = \begin{pmatrix} A_{11}^f & A_{12}^f & A_{16}^f \\ & A_{22}^f & A_{26}^f \\ (sym.) & & A_{66}^f \end{pmatrix} \begin{pmatrix} \gamma_{11}^{f0} \\ \gamma_{22}^{f0} \\ 2\gamma_{12}^{f0} \end{pmatrix} \quad (A12)$$

$$\begin{pmatrix} M_{11}^f \\ M_{22}^f \\ M_{12}^f \end{pmatrix} = \begin{pmatrix} D_{11}^f & D_{12}^f & D_{16}^f \\ & D_{22}^f & D_{26}^f \\ (sym.) & & D_{66}^f \end{pmatrix} \begin{pmatrix} \kappa_{11}^f \\ \kappa_{22}^f \\ \kappa_{12}^f \end{pmatrix}$$

where A_{ij}^f and D_{ij}^f are the coefficients of the laminae stiffness matrices obtained in the usual manner by integration of the corresponding components of the reduced three-dimensional stiffness matrix. The core stress resultants are related in a similar manner to the transverse shear and transverse normal core mid-surface strains:

$$\begin{pmatrix} N_{33}^c \\ N_{23}^c \\ N_{13}^c \end{pmatrix} = \begin{pmatrix} A_{33}^c & 0 & 0 \\ & A_{44}^c & 0 \\ (sym.) & & A_{55}^c \end{pmatrix} \begin{pmatrix} \gamma_{33}^{c0} \\ 2\gamma_{23}^{c0} \\ 2\gamma_{13}^{c0} \end{pmatrix} \quad (A13)$$

where the stiffness coefficients A_{ij}^c are obtained in a similar manner as the face sheet stiffness components A_{ij}^f from the integration of the corresponding components of the three-dimensional stiffness matrix of the core layer with respect to the layer thickness.

Numerical solution procedure

The edge lengths with respect to the x_1 and x_2 axis are denoted by l_1 and l_2 , respectively. The sandwich panel is assumed to be simply supported along all its edges. Thus, transverse displacements \hat{u}_3 as well as the bending moments \hat{M}_{mn} along the external edges are assumed to vanish. With respect to the tangential directions, either the normal edge loads $N_{nn} = \hat{N}_{nn}$ or the corresponding displacements $u_n = \hat{u}_n$ are prescribed. In the present analysis, the latter case of boundary conditions (immovable edges in the tangential plane and normal to the edge directions) is adopted.

Under these conditions, an appropriate representation of transverse displacements is given by

$$u_3^a(x_\alpha, t) = w_{mn}^a(t) \sin(\lambda_m^a x_1) \sin(\mu_n^a x_2), \quad \lambda_m^a = \frac{m\pi}{l_1},$$

$$\mu_n^a = \frac{n\pi}{l_2}$$

$$u_3^d(x_\alpha, t) = w_{pq}^d(t) \sin(\lambda_p^d x_1) \sin(\mu_q^d x_2), \quad \lambda_m^d = \frac{p\pi}{l_1},$$

$$\mu_n^d = \frac{q\pi}{l_2} \quad (A14)$$

where m and n are the number of modal waves with respect to the x_1 and x_2 directions, whereas the numbers of modal waves of the face wrinkling motion are denoted by p and q . The only remaining

unknown quantities with respect to the transverse displacements are the modal amplitudes w_{mn}^a and w_{pq}^d .

The initial geometric imperfections are assumed in the same form as the transverse displacements with the same numbers m , n , p , and q of modal waves

$$\hat{u}_3^a = \hat{w}_{mn}^a \sin(\lambda_m^a x_1) \sin(\mu_n^a x_2), \quad \lambda_m^a = \frac{m\pi}{l_1}, \quad \mu_n^a = \frac{n\pi}{l_2}$$

$$\hat{u}_3^d = \hat{w}_{pq}^d \sin(\lambda_p^d x_1) \sin(\mu_q^d x_2), \quad \lambda_p^d = \frac{p\pi}{l_1}, \quad \mu_q^d = \frac{q\pi}{l_2} \quad (A15)$$

In this case, the modal amplitudes \hat{w}_{mn}^a and \hat{w}_{pq}^d are prescribed quantities that remain constant during the loading history. For the buckling problem, the representation (A15) of geometric imperfections is known to provide the most critical conditions.

A solution for the in-plane displacement u_α^a and u_α^d , which is consistent with the assumed form (A14) of the transverse displacements, can be obtained from the first two equations of motion (A2) and (A3) (that involve, in fact, four equations) used in conjunction with the related constitutive equations (see Hohe and Librescu 2003 and Hause et al. 1998 for details). As a result, a consistent solution for the displacement field $u_i^a(x, t)$, $u_i^d(x, t)$ is available where the modal amplitudes $w_{mn}^a(t)$ and the face wrinkling mode amplitudes $w_{pq}^d(t)$ are the only remaining unknowns. The solution satisfies identically the first four equations of motion (A2) and (A3) as well as the essential boundary conditions. The nonessential boundary conditions are satisfied in an integral average sense along the respective external edges.

The unknowns w_{mn}^a and w_{pq}^d are determined by means of an extended Galerkin procedure (Hause et al. 1998). Therefore, the solution for the displacement field enables one to be substituted into the constitutive equations to obtain the expressions of stress resultants $N_{\alpha\beta}^t$, $N_{\alpha\beta}^b$, $M_{\alpha\beta}^t$, $M_{\alpha\beta}^b$, and N_{i3}^c of the top and bottom face sheets, and of the core, respectively. All these are substituted into the variational equation (A1), and the virtual displacements δu_i^a and δu_i^d are expressed in terms of the variations δw_{mn}^a and δw_{pq}^d of the modal amplitudes. Subsequently, the integration in equation (A1) is performed and the coefficients for the variations δw_{mn}^a and w_{pq}^d of the modal amplitudes are collected. This result is a single homogeneous linear equation for the variations of the modal amplitudes. Since the variations δw_{mn}^a and δw_{pq}^d are arbitrary and independent from each other, the corresponding coefficients must vanish independently.

By this procedure, a system of two linear differential equations for the deformation history in terms of the two unknown modal amplitudes w_{mn}^a and w_{pq}^d and the corresponding accelerations is obtained. The system has the following structure:

$$\ddot{w}_{mn}^a(t) = \sum_{i=0}^3 \sum_{j=0}^3 C_{ij}^a(t) [w_{mn}^a(t)]^i [w_{pq}^d(t)]^j$$

$$\ddot{w}_p^d(t) = \sum_{i=0}^3 \sum_{j=0}^3 C_{ij}^d(t) [w_{mn}^a(t)]^i [w_{pq}^d(t)]^j \quad (A16)$$

where t denotes the time variable. The coefficients $C_{ij}^a(t)$ and $C_{ij}^d(t)$ are lengthy expressions depending on the material properties, on the panel geometry, as well as on the external loading time-history. The obtained initial value problem is solved numerically using an explicit fourth-order Runge-Kutta scheme with variable time increments.